Atmos. Chem. Phys. Discuss., 15, 4879–4907, 2015
www.atmos-chem-phys-discuss.net/15/4879/2015/
doi:10.5194/acpd-15-4879-2015

Atmospheric Chemistry and Physics Discussions
Open Access

Increasing Arabian dust activity and the Indian Summer Monsoon

F. Solmon[1], **V. S. Nair**[2], **and M. Mallet**[3]

[1]The Abdus Salam International Center for Theoretical Physics, Strada Costiera 11, 34100 Trieste, Italy
[2]Space Physics Laboratory Vikram Sarabhai Space Centre Thiruvananthapuram Kerala, 695 022, India
[3]Laboratoire d'Aerologie CNRS, Universite Paul Sabatier, 14 av, Edouard Belin, 31400 Toulouse, France

Received: 6 January 2015 – Accepted: 1 February 2015 – Published: 20 February 2015

Correspondence to: F. Solmon (fsolmon@ictp.it)

Published by Copernicus Publications on behalf of the European Geosciences Union.

Increasing Arabian dust activity and the Indian Summer Monsoon

F. Solmon et al.

Abstract

Over the past decade, Aerosol Optical Depth (AOD) observations based on satellite and ground measurements have shown a significant increase over Arabia and the Arabian Sea, attributed to an intensification of regional dust activity. Recent studies have also suggested that west Asian dust forcing could induce a positive response of Indian monsoon precipitations on a weekly time scale. Using observations and a regional climate model including interactive slab ocean and dust aerosol schemes, the present study investigates possible climatic links between the increasing June-July-August-September (JJAS) Arabian dust activity and precipitation trends over southern India during the 2000–2009 decade. Meteorological reanalysis and AOD observations suggest that the observed decadal increase of dust activity and a simultaneous intensification of summer precipitation trend over southern India are both linked to a deepening of JJAS surface pressure conditions over the Arabian Sea. We show that the model skills in reproducing this trends and patterns are significantly improved only when an increasing dust emission trend is imposed on the basis of observations. We conclude that although climate variability might primarily determine the observed regional pattern of increasing dust activity and precipitation during the 2000–2009 decade, the associated dust radiative forcing might however induce a critical dynamical feedback contributing to enhanced regional moisture convergence and JJAS precipitation over Southern India.

1 Introduction

Indian summer Monsoon rainfall determines to a large extent food production for subcontinental India and has major socio-economic implications. Simulating monsoon precipitations variability from intra-seasonal to inter-annual time scales is identified as major challenge, especially in the context of climate change and increasing anthropogenic pressures over the Indian subcontinent (Lau et al., 2008). The complexity of

ACPD
15, 4879–4907, 2015

the monsoon system arises from the interactions between physical processes involving atmosphere, land and ocean and operating over a wide range of spatial and temporal scales (Turner et al., 2012). The role of aerosol as a possible factor modifying these interactions, with consequences on precipitation variability, has been a subject of intense study for the last decade.

There are basically two mechanisms invoked when discussing the climatic response to direct aerosol forcing over southern Asia. The "solar dimming effect" (Ramanathan et al., 2005) proposes that the reduction in surface solar radiation due to absorption and scattering by aerosols, which shows a regional maximum over northern India and Indian ocean, induces a reduction of the north–south surface temperature gradients resulting in a weakening of the Indian summer monsoon. Consistently with this mechanism, the observed summertime drying trend observed over Central Indian region since 1950 has been attributed to increased anthropogenic aerosol emissions through a slowdown of the tropical meridional circulation (Bollasina et al., 2011). In contrast the "elevated heat pump effect" (Lau et al., 2006) proposes that radiative heating anomalies due to anthropogenic black carbon (BC) and dust transported over the Himalayan foothill and Tibetan plateau during the dry season and the pre-monsoon enhance meridional tropospheric temperature gradients resulting in a strengthening and earlier onset of the Indian monsoon rainfall. Though apparently antagonistic both these mechanisms might be effective at different stage of the pre-monsoon and monsoon development (Meehl et al., 2008) outlining the complexity of aerosol climate feedbacks operating on different time scales. In addition it has been outlined that the regional impact of Asian aerosol might be reinforced by non Asian sources through long distance transport and global dynamical adjustments (Bollasina et al., 2013; Ganguly et al., 2012; Cowan et al., 2011; Wang et al., 2009).

Despite a large focus on anthropogenic aerosol effects justified by the observed intensification of emissions contributing to the "Asian brown cloud" (Ramanathan et al., 2005), the potential importance of natural, and in particular dust aerosol has been also recently highlighted (Jin et al., 2014; Vinoj et al., 2014): it is suggested that west Asian

ACPD
15, 4879–4907, 2015

dust outbreaks can induce a fast and regional atmospheric response which could explain observed positive correlation between aerosol optical depth (AOD) over west Asia and summer precipitation over India on a weekly time scale. Using global circulation model (GCM) experiments with prescribed sea surface temperature (SST) (Vinoj et al., 2014) attributes the cause of this correlation to the large radiative heating induced by dust radiation absorption over Arabia and the Arabian sea resulting in an intensification of south-westerly moisture convergence towards India. This mechanism involves primarily direct and semi-direct aerosol effects and based on a fast reaction of monsoonal weather systems to dust radiative heating perturbation.

The question of characterizing the impact of west Asian dust on Indian monsoon becomes even more relevant if we consider another striking fact which is the observed recent enhancement of Arabian dust activity as measured by satellite and ground based AOD observations during the past decade. Based on Sea-viewing Wide Field of View Sensor (SeaWIFS) satellite observations, significant June-July-August (JJA AOD linear trend reaching 0.014 yr^{-1} over the Arabian region has been determined for the period 1998–2010 (Hsu et al., 2012). This regional trend, associated to a regional increase of dust storm activity, is also detected in ground based photometer measurements from the Aerosol Robotic Measurement Network (AERONET) at Solar village site in Saudi Arabia (Xia, 2011). To our knowledge, the attribution of this regional emission increase to climatic factors and/or land use change is yet to be fully investigated (we indicate later some possible connections with the evolution low pressure conditions over the Arabian sea and the Indian monsoon system).

In this context, the question we wish to primarily address here is: to which extent the recent enhancement of dust activity in the Arabian region could affect the Indian monsoon dynamics and precipitations on decadal time scale? As dust emissions might evolve naturally or/and as a result of climate and land use change (Mahowald, 2007; Mulitza et al., 2010), characterizing and quantifying the regional climate implications of observed dust variability is especially relevant for a better understanding of the Indian monsoon system variability and its possible evolution.

ACPD
15, 4879–4907, 2015

Toward this goal, we use a 50 km resolution regional climate model coupled to an aerosol scheme and a slab-ocean model together with diverse observation and reanalysis products. A specific attention is paid to the quality of the simulated Indian monsoon circulation and precipitation fields as well as to the representation of aerosols notably in term of sources, optical depth, radiative forcing and heating rates gradients. In our approach, we believe that the simulation domain size is large enough to capture important regional dynamical feedbacks to the aerosol radiative perturbation. As a caveat we acknowledge that large scale dynamical feedbacks arising from the possible aerosol induced excitation of planetary waves cannot be accounted for using a limited area model. Knowing in which proportion the effective regional climatic response to aerosol forcing is primarily dominated by regional vs. global dynamical adjustments is however a matter of debate (Ramanathan et al., 2005; Bollasina et al., 2011; Ganguly et al., 2012; Cowan et al., 2011). In Sect. 2 we detail the modeling experiments as well as the different data sets and method use for trend calculation. Dust radiative and climatic impacts and the possible links between Arabian dust trend and the monsoon variability at the decadal scale are then addressed in Sects. 3.

2 Data and methods

2.1 Regional climate model

We use the International Center for Thoretical Physics (ICTP) regional climate model RegCM4 (Giorgi et al., 2012) at 50 km resolution. Runs are performed on the COordinated Regional climate Downscaling Experiment (CORDEX)-India domain over the period 1999–2009 including a 1 year spin up. Boundary conditions are provided by ERA-Interim reanalyzes through a 1000 km buffer zone. Important physical options we used for these study are the Community Land Model version 3.5 (CLM3.5) (Tawfik et al., 2011), the University of Washington turbulence scheme (O'Brien et al., 2012) and the Emanuel convection scheme (Emanuel, 1991) with enabled tracer transport capabili-

ACPD
15, 4879–4907, 2015

ties. The RegCM4 aerosol scheme includes a representation of anthropogenic sulfates, black and organic carbon (Solmon et al., 2006; Qian et al., 2001) as well as sea-salt and dust aerosols. For anthropogenic emissions, we use the Regional Emission inventory in ASia (REAS) (Ohara et al., 2007; Nair et al., 2012) completed by the Atmospheric Chemistry and Climate Model Intercomparison Project (ACCMIP) emissions (Lamarque et al., 2010) to account for biomass burning emissions and REAS-uncovered regions. For natural particles sea salt aerosol emissions are calculated on line and are represented by two (sub and super-micronic) different bins (Zakey et al., 2008). The dust emission scheme (Marticorena et al., 1995; Zakey et al., 2006) includes updates of soil texture distribution (Menut et al., 2013) and emission size distribution (Kok, 2011; Nabat et al., 2012). Lateral Boundary conditions for aerosols are prescribed from a decadal climatology obtained from global runs performed using CAM-Chem model (J. von Hardenberg, personal communication, 2014). Dusts are represented using 4 bins and are impacting short and long wave radiation transfer (Table S1). All other aerosols impact the RegCM shortwave radiation scheme through pre-calculated optical properties (Solmon et al., 2006). Only the first indirect effect is accounted for and applied to sulfate aerosol (Giorgi et al., 2003).

Of particular importance for studying aerosol effects (Zhao et al., 2011), we implemented for this study in ReGCM4 a "flux corrected" slab ocean parameterization following an approach used in the FMS model (http://www.gfdl.noaa.gov/fms-slab-ocean-model-technical-documentation). This parameterization assumes a 50 m depth ocean mixed layer for which we calculate a prognostic SST through a simple energy budget. The lack of ocean dynamics, diffusion and convection, but also other model surface flux errors are compensated by specifying surface flux adjustments (q-flux adjustments) to the slab temperature tendency equation, notably in order to maintain a SST seasonal cycle as close as possible to observations. To derive the q-flux terms, we perform first a "restoring run" (with no interactive dust aerosol) where the slab prognostic SST are restored to observations, taken here as the Optimum Interpolation Sea Surface Temperature (OISST) (Reynolds et al., 2002), and considering a 5

ACPD
15, 4879–4907, 2015

day restoring time scale. As the slab mixed layer model is integrated (over the 1999–2009 period in this experiment), the restoring heat fluxes (q-flux) calculated through this procedure are archived and are saved in a monthly mean climatology at the end of the restoring run. Once the q-flux climatology has been derived, the control and experimental "adjusted runs" are performed accounting for q-fluxes (prescribed from the climatology) in the slab ocean temperature equation. Over the domain, seasonal average differences of SST between the q-flux adjusted control experiment and OISST observations varies in the range of −1 to 1°, ensuring that prognostic SSTs in the adjusted runs do not diverge much from observations and follow a realistic seasonal cycle. This approach extends previous aerosol regional climate studies based on forced SST over the Indian Monsoon and other domains (e.g. Das et al., 2014).

The control experiment consist in a three ensemble members of adjusted runs with no interactive dust aerosol activated (*nodust*). An ensemble of three adjusted runs is then performed with activation of dust (*dust*). An additional three ensemble members run is made with imposing an increasing trend to better reproduce observed AOD trends (*dust_ft*). This is done by increasing the saltation flux erodibility factor (Marticorena et al., 1995) during the run. From year 2004 to 2009 the corresponding increase of erodibility factor is about 30 % and will be illustrated further. In order to limit the effect of internal variability on our analysis of the aerosol feedbacks, we impose a small random perturbation in boundary conditions to every ensemble members during the run following (O'Brien et al., 2011). Results, figures and discussion are based on ensemble means.

2.2 Aerosol Optical Depth trend calculation

JJAS AOD linear trend calculation are first performed using the Sea-viewing Wide Field of View Sensor (SeaWIFS) monthly AOD (550 nm) products at 0.5° and regrided on the 50 km RegCM grid. Algorithms and validity of AOD retrievals from SeaWIFS atmospheric corrections are discussed in Sayer et al. (2012a, b). Moreover, as argued in Hsu et al. (2012), SeaWIFS AOD product is recognized as a "stable" data set min-

ACPD
15, 4879–4907, 2015

imizing sensor calibration impact on trend analysis For each model grid column, the Seawifs AOD are first deseazonalised applying a 13-term moving average for trend first guess and a stable seasonal filter for removing of the seasonal cycle (Brockwell et al., 2002). The deseasonalized times series of JJAS 2000–2009 are then extracted and a linear regression is applied on this subset to determine the JJAS linear trend. Statistical significance of the trend is determined using a F test and we plot only statistically significant pixels with a significant non zero slope (p value < 0.05). Over our region of interest this treatment shows much consistency with the results of Hsu et al., 2012 (Hsu et al., 2012). The same method is applied to simulated monthly AOD time series for model–measurement comparison. Over the particular location of Solar Village, the deseasonalized JJAS AOD time series is also calculated from the Aerosol Robotic Network (AERONET) monthly optical depths and considering the spectral average of AOD at 440 and 640 nm.

2.3 Precipitation trend calculation

For recent 2000–2009 precipitation trend calculation over southern India (Fig. 1b), we used the University of East Anglia Climate Research Unit product (CRU) (Harris et al., 2014), the Tropical Rainfall Measuring Mission (TRMM 3B42) (Huffman et al., 1995) product, the University of Delaware product (UDEL) (Matsuura et al., 2009) and the Precipitation Estimation from Remotely Sensed Information using Artificial Neural Networks (PERSIANN) (Ashouri et al., 2014) product. For each data set, precipitation monthly time series are first geographically averaged over a continental southern Indian box (5–20° N, 60–80° E). Deseasonalized time series are produced following a similar method than for AOD deaseasonalization. A yearly series of JJAS average precipitation is then produce by averaging the different deseaonalized series from each data sets, and keeping the minimum and maximum values for estimation of the spread between different observation data sets.

ACPD
15, 4879–4907, 2015

3 Results and discussion

3.1 Simulation of mean JJAS climate

In this section we assess the model capacity to simulate the mean observed JJAS monsoon circulation and precipitation over the domain. Comparison of simulated JJAS 850 hPa circulation patterns show an overall consistency with ERA-Interim reanalysis in term of pattern and intensity as illustrated in Fig. 1a and b. The main differences are a moderate underestimation of Easterly circulation in the region of the Somalian Jet, and a tendency for the model to overestimate circulation intensity over the Bengal gulf and Indonesia. Model mean JJAS precipitations are evaluated using TRMM, PERSIANN (described in Sect. 2) and the high resolution APHRODITE data set (Yatagai et al., 2012). Variability between observations is illustrated on Fig. 2b, e and g. As in many modeling studies and due to the complexity of convective and dynamics processes, important precipitation overestimation biases are found in region of low precipitation as well as over the North Eastern Himalayas and over the southern Bay of Bengal (Fig. 2). Over continental India, the control simulation (*nodust*) tends to produce drier conditions than observed, with a relative bias increasing toward Eastern and Southern India (Fig. 2d, f and h). The model shows better results when compared to the high resolution APHRODITE rain gauge based data set (Fig. 2g and h). Comparison of Fig. 2b, d, f and h shows that radiative effects of dust tends to reduce model biases over continental India southern and northwestern regions. Overall the simulated mean circulation and precipitation biases obtained in these simulations are either lower, or comparable with CMIP5 state of the art GCMs and multi model ensemble (Sperber et al., 2013).

ACPD
15, 4879–4907, 2015

3.2 Simulation of mean JJAS aerosol optical depth, radiative forcings and heating rates

The climate response to aerosol via direct and semi direct effect is strongly dependant on radiative forcing gradient as well as the vertical distribution of radiative heating due to aerosol. To evaluate model performance in this regard, the AOD simulated for both anthropogenic and natural aerosol is evaluated using the Multiangle Imaging Spectro-Radiometer (MISR) (Martonchik et al., 2004) and SeaWIFS products described in Sect. 2 (Fig. 3). Simulated AOD in regions dominated by anthropogenic emissions (North Eastern India, China, Indonesia) are reasonably captured despite local underestimations for Indian and Chinese megacities. An underestimation of simulated AOD over the Bay of Bengal is however noted, which can be due to uncertainties in emissions, notably for biomass burning (Streets et al., 2003), and/or an excessive deposition rate due overestimated precipitations as discussed previously. Overall, simulated JJAS 2000–2009 AOD shows a very good agreement with observations both in term of magnitude and spatial gradients, providing additional regional details when compared to existing GCM simulations (e.g. Vinoj et al., 2014; Bollasina et al., 2011; Lau et al., 2006). Of particular importance, the dust dominated regions of Arabian peninsula, the Arabian sea and the Indo-Pakistanese desert regions are quite accurately represented in terms of averaged JJAS AOD. Over these regions, the net dust surface radiative forcing (Fig. 4a) is dominated by shortwave cooling vs. positive long-wave surface warming which is reported on Supplement (Fig. S1). This induces a surface temperature cooling illustrated on Fig. 4b which can reach -2 K in sub-regions of Arabia. Over the ocean, a surface cooling is also obtained through the slab ocean response, but tends to be less effective due to larger surface thermal inertia. SST cooling reaches up to $-1\,^{\circ}$C close to Oman Gulf with a decreasing gradient towards India (Fig. 4b). As a result of both dust optical properties and surface albedo, top of atmosphere radiative forcing (TOA) is mostly positive over the high emission region of Arabian peninsula, and becomes negative above the ocean and continental India. In comparison to Arabian penisnsula,

ACPD
15, 4879–4907, 2015

the TOA radiative forcing efficiencies (i.e. TOA normalized by AOD) shows relatively less of a warming effect in the Indo-Pakistanese and Northern India desert regions due to lower surface albedo. Atmospheric radiative heating rate anomalies primarily associated to dust radiative absorption, are presented on Figs. 4d and S2. Mean simulated values for JJAS ranges from more than 1 $K day^{-1}$ over source regions of Arabia to about 0.3 $K day^{-1}$ in the core of the Arabian dust outflow, located between 850 and 600 hPa. Over India, the JJAS dust radiative warming at 850hp reaches about 0.05 to 0.1 $K day^{-1}$. These values are in the range of different observational studies (Moorthy et al., 2009; Kuhlmann et al., 2010; Nair et al., 2008). We note that when radiative and moist processes feedbacks are combined, the diabatic heating induced by dust is however significantly lower than the 2 $K day^{-1}$ warming reported in Vinoj et al. (2014) which can also explain differences discussed Sect. 4.

3.3 Mean monsoon response to dust radiative forcing

Regional climate adjustments to dust radiative forcing are first discussed by comparing "*dust*" and "*nodust*" simulations for JJAS 2000–2009. Figure 5 presents 850 hPa circulation and geopotential height (GPH) anomalies induced by dust direct and semi-direct over the domain. Two patterns emerge from this comparison: the first one is a low GPH anomaly centered over southern Arabian Peninsula associated to a cyclonic circulation, and the second one a positive GPH anomaly roughly centered over North Eastern India associated to an anti-cyclonic anomaly. Regions of large positive or negative values in 850 hPa GPH difference patterns tend to match pretty closely the regional TOA radiative forcing patterns (Figure. 4b). Over Arabia, dust radiative warming is maximum due to high concentration of dust while dust surface cooling efficiency is relatively reduced due to high surface albedo. This induces a deepening of the Arabian thermal low (Fig. 5) and dry convection collocated with the maximum of dust radiative warming (Fig. S2c and d). On its southern part, the cyclonic circulation anomaly is associated to an intensification of the Somalia jet and Eastward circulation between 10 and 20° N and 50 to 75° E. This intensification induces an enhanced convergence of moisture flux

ACPD
15, 4879–4907, 2015

toward southern India and an increase of convective activity and precipitations over the southern Indian continent (Figs. 5 and S2d and e). From these simulations we estimate that this mechanism could enhance average precipitation by up to 10 % in southern India thus contributing to improve the model dry bias (Fig. 2a). Up to roughly 20° N, our results show much similarity with GCM results notably reported in Vinoj et al. (2014). One noticeable difference however is, while Vinoj et al. (2014) obtain an increase of precipitation over northern Arabian sea, north western India and Pakistan, convective precipitation tend to be inhibited for these regions in our case. This regional stabilization is induced by a relatively large surface radiative dimming which decreases continental and sea surface temperatures (Fig. 4c), and for which inhibiting effect on convection is predominant over dust absorption radiative warming, consistently with a negative simulated TOA radiative forcing (Fig. 4b). On average, the Arabian and Indo Pakistanese dust sources appear to have a dual signature resulting in strengthening the Somalian jet, moisture convergence and precipitation over southern India, while inhibiting convective precipitation and decreasing monsoon intensity north of about 20° N (Fig. 5). Several factors such as soil nature and aerosol transport distance from the sources contribute to shape out regional contrast in dust radiative forcing and associated convective and dynamical responses. For example in our simulations, the regional surface albedo is higher over Arabia compared to the Indo Pakistanese and Iran region, resulting in enhanced aerosol radiative heating efficiency over Arabia. Fine dust transported from Arabian, Indo Pakistanese and Iran sources to northern India are relatively diffusive and induce a moderate radiative heating in line with recent observational studies. This, on average, favor a stabilization rather than a "heat pump effect" over convective regions of northern India. That said, it must be noted that radiative forcing and impact also depends on dust chemical composition and absorption/diffusion properties (Solmon et al., 2008), which can exhibit a large regional variability (Deepshikha et al., 2005). In our simulation we do not account for regional variation of dust refractive indices. We also do not account for possible dust indirect effects on warm and ice cloud

ACPD
15, 4879–4907, 2015

microphysics for which there is still a considerable debate and for which regional impact is difficult to assess.

3.4 Coupling of Arabian dust increasing activity and precipitation variability over the 2000–2009 decade

Our work hypothesis is that, if the above mechanisms are valid, the observed increasing dust AOD trend over Arabia over the decade 2000–2010 might have been associated with a positive impact on circulation and precipitation over southern India. Linear trends of JJAS AOD, calculated from SeaWIFS observations over our domain (cf. Sect. 2), are presented on Fig. 7. As already reported in Hsu et al. (2012), strong positive trend are found over Arabian Peninsula region. The positive AOD trend observed in the AERONET station of solar village (Xia, 2011) is also reported (Fig. 6a). From the time series in Fig. 6a, we note that the JJAS observed deseasonalized AOD are better represented by a quadratic vs. linear regression, and that the trend tends to steepen around year 2005. Consequently the 2005–2009 pentad (P0509) shows sensibly higher averaged AOD relative to the 2000–2004 pentad (P0004).

An increasing trend for precipitation over southern and eastern India is also detected in several data sets as illustrated in Fig. 6b. In a rather similar way to Arabian AOD, the observed JJAS precipitation in Fig. 6b shows a relative intensification for P0509 relative to P0004. If we plot the mean surface pressure and circulation differences between “dusty P0509” and “less dusty P0004” pentads from ERAI and NCEP2 reanalyzes (Figs. 8a and S3), we observe that both data sets show a cyclonic pattern over the Eastern Arabian sea and India with enhanced southwesterly circulation toward continental India. The associated increase of moisture flow over southern India is a likely reason for enhanced precipitations during P0509 pentad relative to P0004 observed in precipitation data sets on Fig. 6b.

Furthermore, the cyclonic pattern found in pentad differences depicts a relative increase of the frequency/intensity of low pressure situations over northern Arabian sea for P0509 relative to P0004. Such conditions are favorable to enhanced Shamal wind

ACPD
15, 4879–4907, 2015

(Hamidi et al., 2013; Notaro et al., 2013), and could thus be a likely reason for the observed increase of AOD during the decade. On short time scales, it is also known that individual storms moving in the Arabian sea and the northern bay of Bengal can trigger large dust emission from Arabia and the Indo-Pakistanese – Iran desert regions (Kaskaoutis et al., 2014; Ramaswamy, 2014). Based on these observations, both enhanced precipitation over India and Arabian dust AOD increase could be linked to lower pressure conditions prevailing over the Arabian Sea during PO509 relative to P0004 pentads. Reasons for these conditions are likely a feature of climate decadal variability over the region and further analysis is beyond the scope of this study. Note that part of the short time scale AOD/precipitation correlation attributed to dust direct and semi-direct feedbacks (Vinoj et al., 2014) could also be explained by dynamical systems leading to both high dust emissions/transport and heavy precipitations over India on short time scale.

Focusing now on model results we see that, although the standard *dust* simulation is able to capture a slightly positive AOD trend over part of the Arabian Peninsula, this trend nevertheless largely underestimated when compared to observations (Fig. 7a and b). Consistently with the arguments developed before, a likely reason for this underestimation is related to the fact that cyclonic pattern found in reanalyzes pentad difference is also not properly captured by the model as shown in Fig. 8b and c, meaning that the model does not reproduce properly increasing occurrences or/and intensification of Shamal conditions during the decade. These deficiencies are likely to be due to uncertainties in coupled convective and dynamical processes over northern Arabian Sea, Pakistan and Bengal gulf which are extremely challenging to capture properly in climate models (Turner et al., 2012). In terms of dust AOD, the uncertainties in dust emissions parameterizations could further worsen errors in simulating adequately regional climatic trends (Evan et al., 2014).

However, since dust trigger a potentially important climatic feedback over the region, it is possible that failure in capturing the increasing Arabian dust trend contributes also to failure in capturing a proper trend in regional climate. To explore this issue,

ACPD
15, 4879–4907, 2015

Increasing Arabian dust activity and the Indian Summer Monsoon

F. Solmon et al.

we perform an additional experiment where dust emissions are forced in order to reproduce more realistically the observed JJAS AOD increasing trend (see Sect. 2.2 and Figs. 5a and 7b and c). On the JJAS AOD time series (Fig. 5a) we can note that the adjusted model shows enhanced AOD for P0509 pentad relatively to P0004 in a relatively similar way to observations. In term of climatic impact, simulated circulation and surface pressure changes between P0004 and P0509 show a rather different behavior whether considering *nodust*, *dust* only, or adjusted *dust_ft* simulations (cf. Sect. 2), especially over Arabian Sea and southern India (Fig. 8). With no dust, or when dust increasing emission tendency is not forced, the model tends to reproduce an anti-cyclonic pattern over the Arabian Sea (Fig. 8b and c) and no enhanced westward circulation toward the Indian coast, unlike what is observed in reanalyzes (Fig. 8a). When dust tendency is forced however, a westward convergence is obtained between 5 and 20° N, and surface pressure pentad differences over the Arabian sea switch from positive to slightly negative (Fig. 8d). A cyclonic pattern centered over eastern India is even simulated in the dust simulation but of less intensity than seen in the reanalyzes. Bearing in mind model limitations, the simulations tend to show improved circulation changes compared to reanalyzes when dust are present, and especially when the increasing dust trend is more realistically forced. From these results we suggest that while the cyclonic changes observed between pentad in reanalysis might be primarily a feature of climate variability, the likely associated increase in JJAS west Asian dust emission and Arabian sea AOD could however determine an important positive feedback contributing to intensify westerly circulation and humidity flux convergence towards the south-western Indian coast. The simulated impact of this feedback on summer precipitation trends over southern India is depicted on Fig. 5b: simulated JJAS precipitations show an increasing linear trend in *dust_ft* deseasonalized JJAS simulations of about 0.11 $\mathrm{mm\,day^{-1}\,yr^{-1}}$ and close to the value of the JJAS trend calculated from observations (0.13 $\mathrm{mm\,day^{-1}\,yr^{-1}}$), when no statistically significant trends are detected in *nodust* and *dust* simulations.

ACPD
15, 4879–4907, 2015

4 Conclusion

Overall our results emphasize the possible two-way interaction between dust emissions variability and the summer regional climate variability in the Indian monsoon domain for inter-annual to decadal time scale. Using observations and a regional climate model, we suggest that an increasing Arabian dust emission trends could have impacted the Indian monsoon circulation and contributed to explain observed increasing 2000–2009 summer precipitations over southern India. Dust radiative forcing might determine a positive dynamical feedback, favoring the establishment of lower pressure conditions over the Arabian Sea and resulting in both enhanced Arabian dust emissions and precipitation over southern India. The measured dust 2000–2009 AOD trends over Arabia and the Arabian Sea are equally if not more important as AOD trend reported for continental India and attributed to anthropogenic pollution increase (Babu et al., 2013). In view of these results, capturing the positive feedbacks between dynamics and dust emission trend in climate model could lead to a more realistic representation of precipitation decadal variability over India. However, the present study as well as (Evan et al., 2014) show that current dust parametrisation used in climate models show difficulties to reproduce observed regional AOD inter-annual and decadal variability. Improvement of models whether they deal with dust emissions processes, regional land use change and surface wind speed downscaling are thus of primary importance.

The Supplement related to this article is available online at doi:10.5194/acpd-15-4879-2015-supplement.

Acknowledgements. The authors would like to thank Jost von Hardenberg for providing aerosol large scale fields for boundary conditions, R. Farneti and F. Kucharski for advices on slab ocean implementation and scientific discussion as well as G. Giuliani and the RegCM developing team for maintaining and managing the code.

ACPD
15, 4879–4907, 2015

References

Ashouri, H., Hsu, K.–L., Sorooshian, S., Braithwaite, D. K., Knapp, K. R., Cecil, L. D., and Prat, O. P.: PERSIANN-CDR: daily precipitation climate data record from multi-satellite observations for hydrological and climate studies, B. Am. Meteorol. Soc., doi:10.1175/BAMS-D-13-00068.1, 2014.

Babu, S. S., Manoj, M., Moorthy, K. K., Gogoi, M. M., Nair, V. S., Kompalli, S. K., Satheesh, S. K., Niranjan, K., Ramagopal, K., Bhuyan, P. K., and Darshan Singh: Trends in aerosol optical depth over Indian region: potential causes and impact indicators, J. Geophys. Res.-Atmos., 118, 11794–11806, 2013.

Bollasina, M. A., Ming, Y. and Ramaswamy, V.: Anthropogenic aerosols and the weakening of the South Asian summer monsoon, Science, 334, 502–505, 2011.

Bollasina, M. A., Ming, Y., and Ramaswamy, V.: Earlier onset of the Indian monsoon in the late twentieth century: the role of anthropogenic aerosols, Geophys. Res. Lett., 40, 3715–3720, 2013.

Brockwell, P. J. and Davis, R. A.: Introduction to Time Series and Forecasting, Vol. 1, Taylor & Francis, 2002.

Cowan, T. and Cai, W.: The impact of Asian and non-Asian anthropogenic aerosols on 20th century Asian summer monsoon, Geophys. Res. Lett., 38, doi:10.1029/2011GL047268, 2011.

Das, S., Dey, S., and Dash, S. K.: Impacts of aerosols on dynamics of Indian summer monsoon using a regional climate model, Clim. Dynam., 1–13, 2014.

Deepshikha, S., Satheesh, S. K. and Srinivasan, J.: Regional distribution of absorbing efficiency of dust aerosols over India and adjacent continents inferred using satellite remote sensing, Geophys. Res. Lett., 32, L03811–L03811, 2005.

Emanuel, K. A.: A scheme for representing cumulus convection in large-scale models, J. Atmos. Sci., 48, 2313–2329, 1991.

Evan, A. T., Flamant, C., Fiedler, S., and Doherty, O.: An analysis of aeolian dust in climate models, Geophys. Res. Lett., 41, 5996–6001, 2014.

Ganguly, D., Rasch, P. J., Wang, H., and Yoon, J.-H.: Climate response of the South Asian monsoon system to anthropogenic aerosols, J. Geophys. Res.-Atmos., 117, doi:10.1029/2012JD017508, 2012.

ACPD
15, 4879–4907, 2015

Increasing Arabian dust activity and the Indian Summer Monsoon

F. Solmon et al.

Giorgi, F., Bi, X. and Qian, Y.: Indirect vs. direct effects of anthropogenic sulfate on the climate of East Asia as simulated with a regional coupled climate-chemistry/aerosol model, Climatic Change, 58, 345–376 2003.
Giorgi, F., Coppola, E., Solmon, F., Mariotti, L., Sylla, M., Bi, X., and others: RegCM4: model description and preliminary tests over multiple CORDEX domains, Clim. Res., 2, 7–29, 2012.
Hamidi, M., Kavianpour, M. R., and Shao, Y.: Synoptic analysis of dust storms in the Middle East, Asia-Pac. J. Atmos. Sci., 49, 279–286, 2013.
Harris, I., Jones, P., Osborn, T., and Lister, D.: Updated high-resolution grids of monthly climatic observations-the CRU TS3.10 Dataset, Int. J. Climatol., 34, 623–642, 2014.
Hsu, N. C., Gautam, R., Sayer, A. M., Bettenhausen, C., Li, C., Jeong, M. J., Tsay, S.-C., and Holben, B. N.: Global and regional trends of aerosol optical depth over land and ocean using SeaWiFS measurements from 1997 to 2010, Atmos. Chem. Phys., 12, 8037–8053, doi:10.5194/acp-12-8037-2012, 2012.
Huffman, G. J. et al.: Global precipitation estimates based on a technique for combining satellite-based estimates, rain gauge analysis, and NWP model precipitation information, J. Climate, 8, 1284–1295, 1995.
Jin, Q., Wei, J., and Yang, Z.-L.: Positive response of Indian summer rainfall to Middle East dust, Geophys. Res. Lett., 4068–4074, 2014.
Kaskaoutis, D., Rashki, A., Houssos, E., Goto, D., and Nastos, P.: Extremely high aerosol loading over Arabian Sea during June 2008: the specific role of the atmospheric dynamics and Sistan dust storms, Atmos. Environ., 94, 374–384, 2014.
Kok, J. F.: A scaling theory for the size distribution of emitted dust aerosols suggests climate models underestimate the size of the global dust cycle, P. Natl. Acad. Sci. USA, 108, 1016–1021, 2011.
Kuhlmann, J. and Quaas, J.: How can aerosols affect the Asian summer monsoon? Assessment during three consecutive pre-monsoon seasons from CALIPSO satellite data, Atmos. Chem. Phys., 10, 4673–4688, doi:10.5194/acp-10-4673-2010, 2010.
Lamarque, J.-F., Bond, T. C., Eyring, V., Granier, C., Heil, A., Klimont, Z., Lee, D., Liousse, C., Mieville, A., Owen, B., Schultz, M. G., Shindell, D., Smith, S. J., Stehfest, E., Van Aardenne, J., Cooper, O. R., Kainuma, M., Mahowald, N., McConnell, J. R., Naik, V., Riahi, K., and van Vuuren, D. P.: Historical (1850–2000) gridded anthropogenic and biomass burning emissions of reactive gases and aerosols: methodology and application, Atmos. Chem. Phys., 10, 7017–7039, doi:10.5194/acp-10-7017-2010, 2010.

ACPD
15, 4879–4907, 2015

Lau, K. M., Kim, M. K., and Kim, K. M.: Asian summer monsoon anomalies induced by aerosol direct forcing: the role of the Tibetan Plateau, Clim. Dynam., 26, 855–864, 2006.
Lau, K. M. et al.: The Joint Aerosol-Monsoon Experiment: a new challenge for monsoon climate research, B. Am. Meteorol. Soc., 89, 369–383, 2008.
Mahowald, N. M.: Anthropocene changes in desert area: Sensitivity to climate model predictions, Geophys. Res. Lett., 34, doi:10.1029/2007GL030472, 2007.
Marticorena, B. and Bergametti, G.: Modeling the atmospheric dust cycle: 1. Design of a soil-derived dust emission scheme, J. Geophys. Res.-Atmos., 100, 16415–16430, 1995.
Martonchik, J. V., Diner, D. J., Kahn, R., Gaitley, B., and Holben, B. N.: Comparison of MISR and AERONET aerosol optical depths over desert sites, Geophys. Res. Lett., 31, doi:10.1029/2004GL019807, 2004.
Matsuura, K. and Willmott, C. J.: Terrestrial precipitation: 1900–2008 gridded monthly time series, Center for Climatic Research Department of Geography Center for Climatic Research, University of Delaware, 2009.
Meehl, G. A., Arblaster, J. M., and Collins, W. D.: Effects of black carbon aerosols on the Indian monsoon, J. Climate, 21, 2869–2882, 2008.
Menut, L. et al.: Impact of surface roughness and soil texture on mineral dust emission fluxes modeling, J. Geophys. Res.-Atmos., 118, 6505–6520, 2013.
Moorthy, K. K., Nair, V. S., Babu, S. S., and Satheesh, S.: Spatial and vertical heterogeneities in aerosol properties over oceanic regions around India: implications for radiative forcing, Q. J. Roy. Meteor. Soc., 135, 2131–2145, 2009.
Mulitza, S., Heslop, D., Pittauerova, D., Fischer, H. W., Meyer, I., Stuut, J.-B., and others.: Increase in African dust flux at the onset of commercial agriculture in the Sahel region, Nature, 466, 226–228, 2010.
Nabat, P., Solmon, F., Mallet, M., Kok, J. F., and Somot, S.: Dust emission size distribution impact on aerosol budget and radiative forcing over the Mediterranean region: a regional climate model approach, Atmos. Chem. Phys., 12, 10545–10567, doi:10.5194/acp-12-10545-2012, 2012.
Nair, V. S, Babu, S. S., and Moorthy, K. K.: Aerosol characteristics in the marine atmospheric boundary layer over the Bay of Bengal and Arabian Sea during ICARB: spatial distribution and latitudinal and longitudinal gradients, J. Geophys. Res.-Atmos., 113, doi:10.1029/2008JD009823, 2008.

Nair, V. S. et al.: Simulation of South Asian aerosols for regional climate studies, J. Geophys. Res.-Atmos., 117, doi:10.1029/2011JD016711, 2012.
Notaro, M., Alkolibi, F., Fadda, E., and Bakhrjy, F.: Trajectory analysis of Saudi Arabian dust storms, J. Geophys. Res.-Atmos., 118, 6028–6043, 2013.
O'Brien, T. A, Sloan, L. C., and Snyder, M. A.: Can ensembles of regional climate model simulations improve results from sensitivity studies?, Clim. Dynam., 37, 1111–1118, 2011.
O'Brien, T. A., Chuang, P. Y., Sloan, L. C., Faloona, I. C., and Rossiter, D. L.: Coupling a new turbulence parametrization to RegCM adds realistic stratocumulus clouds, Geosci. Model Dev., 5, 989–1008, doi:10.5194/gmd-5-989-2012, 2012.
Ohara, T., Akimoto, H., Kurokawa, J., Horii, N., Yamaji, K., Yan, X., and Hayasaka, T.: An Asian emission inventory of anthropogenic emission sources for the period 1980–2020, Atmos. Chem. Phys., 7, 4419–4444, doi:10.5194/acp-7-4419-2007, 2007.
Qian, Y., Giorgi, F., Huang, Y., Chameides, W., and Luo, C.: Regional simulation of anthropogenic sulfur over East Asia and its sensitivity to model parameters, Tellus B, 53, 171–191, 2001.
Ramanathan, V., Chung, C., Kim, D., Bettge, T., Buja, L., Kiehl, J., Washington, W. M., Fu, Q., Sikka, D. R., and Wild, M.: Atmospheric brown clouds: impacts on South Asian climate and hydrological cycle, P. Natl. Acad. Sci. USA, 102, 5326–5333, 2005.
Ramaswamy, V.: Influence of tropical storms in the Northern Indian Ocean on dust entrainment and long-range transport, in: Typhoon Impact and Crisis Management, Springer, 2014.
Reynolds, R. W., Rayner, N. A., Smith, T. M., Stokes, D. C., and Wang, W.: An improved in situ and satellite SST analysis for climate, J. Climate, 15, 1609–1625, 2002.
Sayer, A. M., Hsu, N. C., Bettenhausen, C., Jeong, M.-J., Holben, B. N., and Zhang, J.: Global and regional evaluation of over-land spectral aerosol optical depth retrievals from SeaWiFS, Atmos. Meas. Tech., 5, 1761–1778, doi:10.5194/amt-5-1761-2012, 2012a.
Sayer, A. M., Hsu, N. C., Bettenhausen, C., Ahmad, Z., Holben, B. N., Smirnov, A., and Zhang, J.: SeaWiFS Ocean Aerosol Retrieval (SOAR): algorithm, validation, and comparison with other data sets, J. Geophys. Res.-Atmos., 117, doi:10.1029/2011JD016599, 2012b.
Solmon, F., Giorgi, F., and Liousse, C.: Aerosol modelling for regional climate studies: application to anthropogenic particles and evaluation over a European/African domain, Tellus B, 58, 51–72, 2006.

ACPD
15, 4879–4907, 2015

Increasing Arabian dust activity and the Indian Summer Monsoon

F. Solmon et al.

Solmon, F., Mallet, M., Elguindi, N., Giorgi, F., Zakey, A., and Konaré, A.: Dust aerosol impact on regional precipitation over western Africa, mechanisms and sensitivity to absorption properties, Geophys. Res. Lett., 35, doi:10.1029/2008GL035900, 2008.

Sperber, K. R., Annamalai, H., Kang, I.-S., Kitoh, A., Moise, A., Turner, A., and Zhou, T.: The Asian summer monsoon: an intercomparison of CMIP5 vs. CMIP3 simulations of the late 20th century, Clim. Dynam., 41, 2711–2744, 2013.

Streets, D. G., Bond, T. C., Carmichael, G. R., Fernandes, S. D., Fu, Q., He, D., and Yarber, K. F.: An inventory of gaseous and primary aerosol emissions in Asia in the year 2000, J. Geophys. Res.-Atmos., 108, doi:10.1029/2002JD003093, 2003.

Tawfik, A. B. and Steiner, A. L.: The role of soil ice in land–atmosphere coupling over the United States: a soil moisture–precipitation winter feedback mechanism, J. Geophys. Res.-Atmos., 116, doi:10.1029/2002JD003093, 2011.

Turner, A. G and Annamalai, H.: Climate change and the South Asian summer monsoon, Nature Climate Change, 2, 587–595, 2012.

Vinoj, V., Rasch, P. J., Wang, H., Yoon, J.-H., Ma, P.-L., Landu, K., and Singh, B.: Short-term modulation of Indian summer monsoon rainfall by West Asian dust, Nat. Geosci., 308–313, 2014.

Wang, C., Kim, D., Ekman, A. M., Barth, M. C., and Rasch, P. J.: Impact of anthropogenic aerosols on Indian summer monsoon, Geophys. Res. Lett., 36, doi:10.1029/2009GL040114, 2009.

Xia, X.: Variability of aerosol optical depth and Angstrom wavelength exponent derived from AERONET observations in recent decades, Environ. Res. Lett., 6, 44011–44019, 2011.

Yatagai, A., Kamiguchi, K., Arakawa, O., Hamada, A., Yasutomi, N., and Kitoh, A.: APHRODITE: constructing a long-term daily gridded precipitation dataset for Asia based on a dense network of rain gauges, B. Am. Meteorol. Soc., 93, 1401–1415, 2012.

Zakey, A. S., Solmon, F., and Giorgi, F.: Implementation and testing of a desert dust module in a regional climate model, Atmos. Chem. Phys., 6, 4687–4704, doi:10.5194/acp-6-4687-2006, 2006.

Zakey, A. S., Giorgi, F., and Bi, X.: Modeling of sea salt in a regional climate model: fluxes and radiative forcing, J. Geophys. Res.-Atmos., 113, doi:10.1029/2007JD009209, 2008.

Zhao, C., Liu, X., Ruby Leung, L., and Hagos, S.: Radiative impact of mineral dust on monsoon precipitation variability over West Africa, Atmos. Chem. Phys., 11, 1879–1893, doi:10.5194/acp-11-1879-2011, 2011.

ACPD
15, 4879–4907, 2015

Increasing Arabian dust activity and the Indian Summer Monsoon

F. Solmon et al.

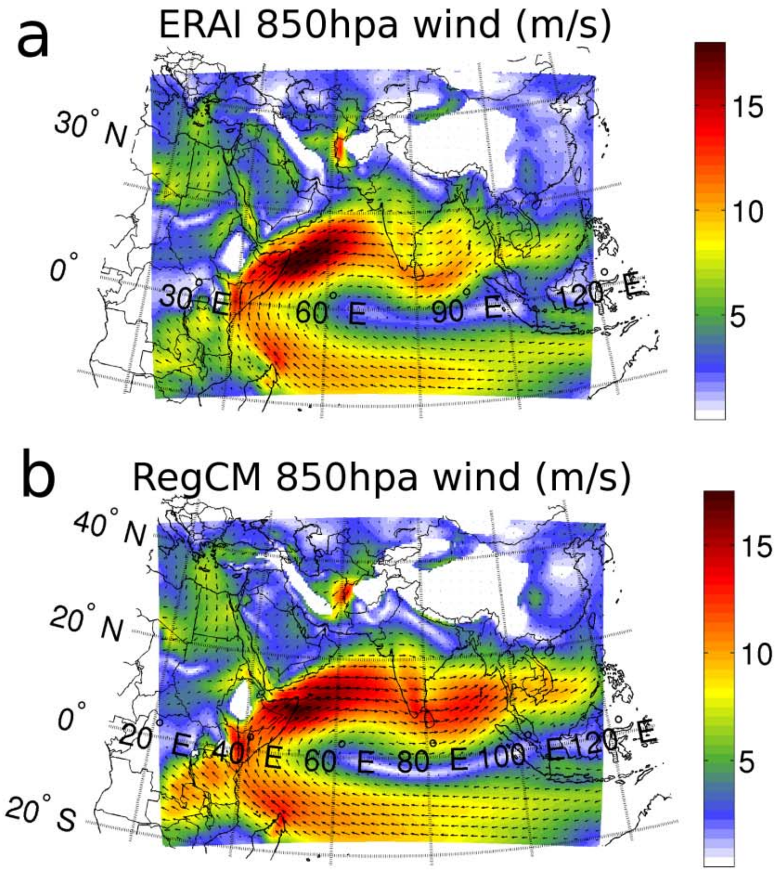

Figure 1. Mean 850 hPa JJAS wind intensity and direction as seen in **(a)** the ERAI reanalysis and **(b)** the RegCM *nodust* simulation for the period 2000–2009 and over the CORDEX-India domain. All modeling results represent a 3 member's ensemble mean.

ACPD
15, 4879–4907, 2015

Increasing Arabian dust activity and the Indian Summer Monsoon

F. Solmon et al.

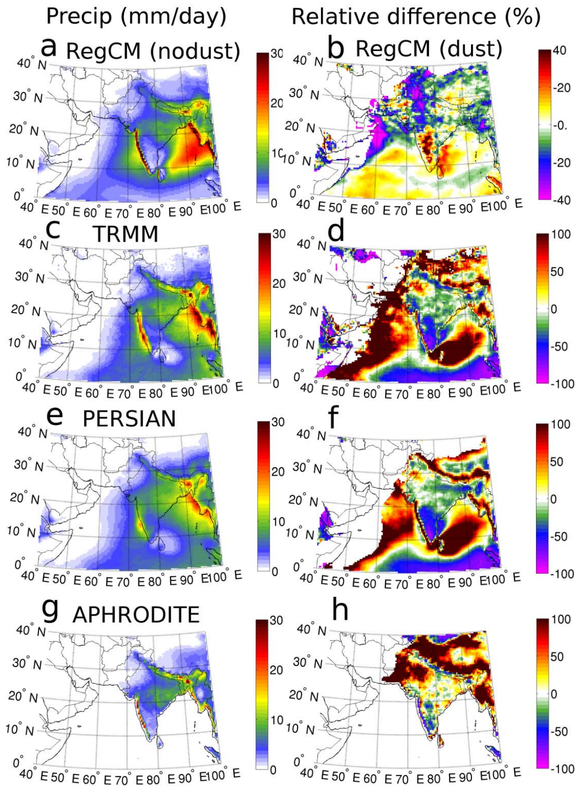

Figure 2. (a) Mean JJAS 2000–2009 precipitation simulated by the model in "*nodust*" configurations. **(b)** Relative difference in precipitation between *dust* and *nodust* simulations for JJAS 2000–2009 and calculated as *(dust –nodust/nodust)* ×100. **(c)** JJAS 2000–2009 TRMM precipitation. **(d)** Relative difference (bias) between *nodust* and TRMM precipitations for observed precipitation level > 0.2 mm day^{-1}. (**e** and **f**) Same than (**c** and **d**) for the PERSIANN data set. (**g** and **h**) Same than (**c** and **d**) for the APHRODITE data sets, but calculated for JJAS 2000–2007 only. All modeling results represent a 3 member's ensemble mean.

ACPD
15, 4879–4907, 2015

Increasing Arabian dust activity and the Indian Summer Monsoon

F. Solmon et al.

Title Page
Abstract | Introduction
Conclusions | References
Tables | Figures
◀| |▶
◀ ▶
Back | Close
Full Screen / Esc
Printer-friendly Version
Interactive Discussion

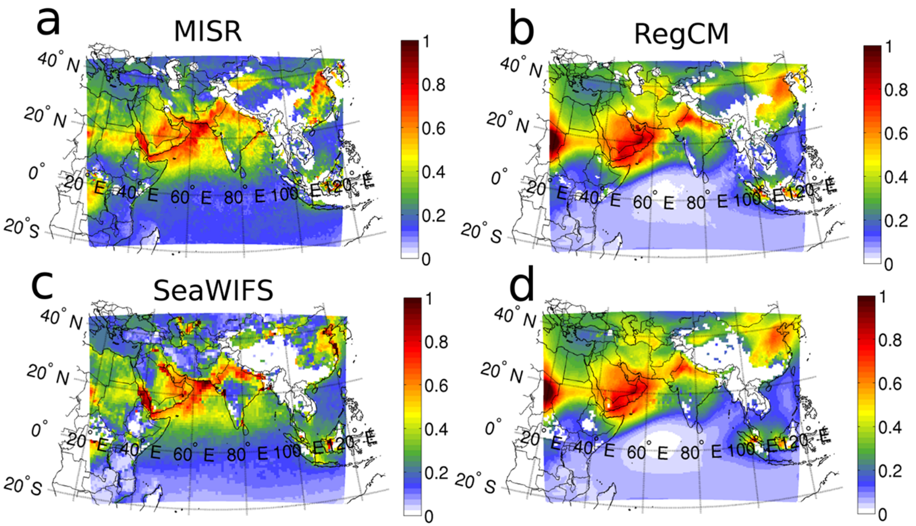

Figure 3. JJAS 2000–2009 AOD seen from the **(a)** MISR sensor and **(b)** as simulated by RegCM "*dust_f*" simulation for the full CORDEX-India domain. JJAS composite averages are built form monthly observations and model outputs. Regions of missing observations are screened out from the model averages (**c** and **d**) Same as (**a** and **b**) for the SeaWIFS observations. All modeling results represent a 3 member's ensemble mean.

ACPD
15, 4879–4907, 2015
Increasing Arabian dust activity and the Indian Summer Monsoon
F. Solmon et al.

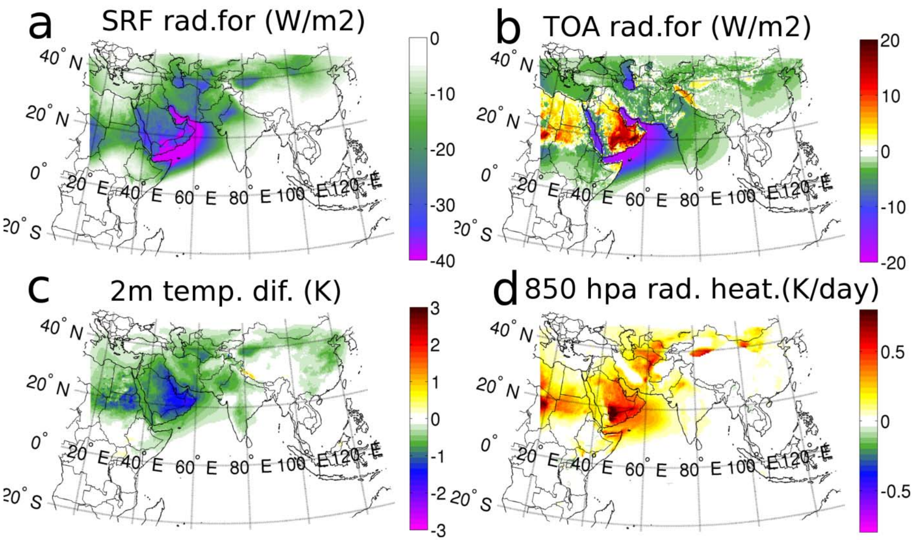

Figure 4. (a) JJAS 2000–2009 Dust aerosol surface radiative forcing diagnostic. **(b)** JJAS 2000–2009 Dust top of atmosphere radiative forcing diagnostic. **(c)** JJAS 2000–2009 2 m temperature difference between *dust* and *nodust* simulations. **(d)** 850 hPa radiative heating rate difference between *dust* and *nodust* simulations. All modeling results represent a 3 member's ensemble mean.

ACPD
15, 4879–4907, 2015

Increasing Arabian dust activity and the Indian Summer Monsoon

F. Solmon et al.

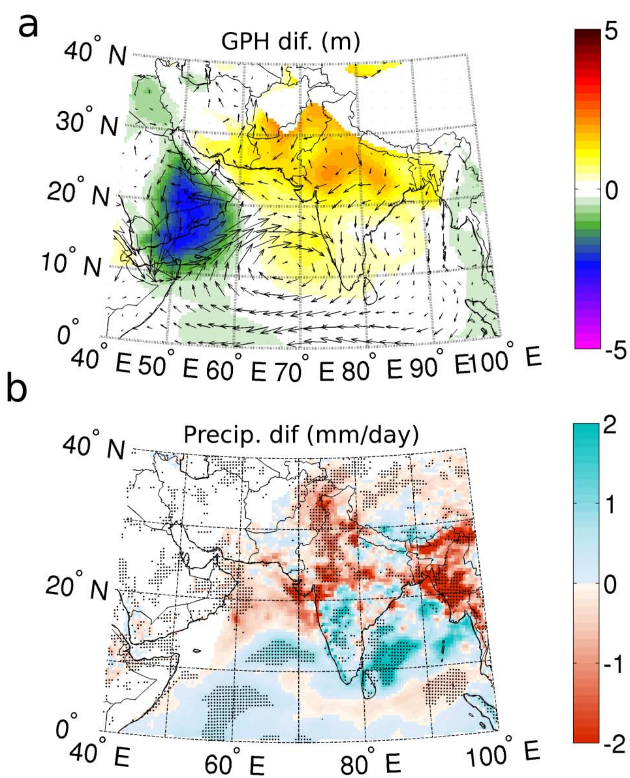

Figure 5. Dust impact on the mean monsoon dynamic and precipitations over the period JJAS 2000–2009. **(a)** 850 hPa geopotential heights (GPH) and monsoon circulation dust induced anomalies calculated as the GPH difference between *dust* and *nodust* simulations. **(b)** Dust induced precipitation anomaly. The dotted region defines statistically significant results at the 95 % confidence level. All modeling results represent a 3 member's ensemble mean.

ACPD
15, 4879–4907, 2015

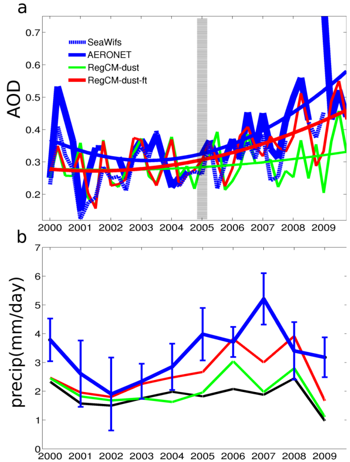

Figure 6. Arabian AOD and Southern India deseasonalized precipitation trends during the decade 2000–2009. **(a)** The thick blue line represents monthly deseasonalised time series of JJAS AOD obtained from the Solar Village AERONET station (monthly product, average of 480–640 nm spectral bands). A quadratic regression fit, showing the progressive intensification of observed dust activity is superimposed (blue curve). The blue hatched line represents the deasesonalised AOD time series obtained from SeaWIFS AOD interpolated on the Solar Village station. The green lines represents the monthly deseasonalized time series (as well as the corresponding quadratic fit) of JJAS AOD simulated by the model in *dust* simulation. The red lines represents the monthly deseasonalized time series (as well as the corresponding quadratic fit) of JJAS AOD simulated by the model with forced dust emission trends (*dust_ft* simulation). **(b)** The blue line represents the yearly time evolution of observed continental precipitation averaged for JJAS, over a southern India box (5–20N; 60–80E) and for different data sets (TRMM, CRU, PERSIANN). The blue bars materialize the amplitude between maximum and minimum values amongst observations for a given year. The equivalent deseasonalized JJAS average simulated precipitations are reported for the *nodust* simulations (black line), the *dust* standard simulations (green line) and the forced emission trend *dust_ft* simulations (red line). All modeling results represent a 3 member's ensemble mean.

ACPD
15, 4879–4907, 2015

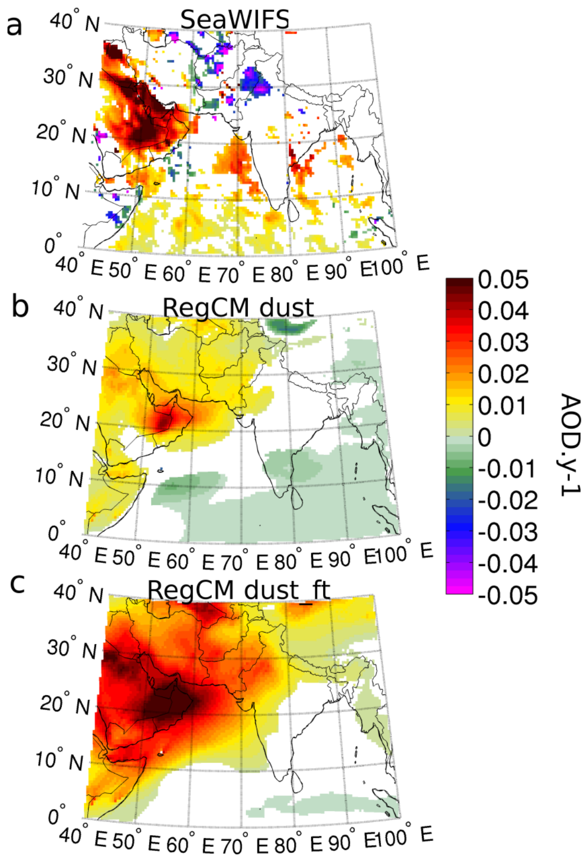

Figure 7. Linear JJAS AOD trend calculated over the 2000–2009 period from: **(a)** SeaWIFS monthly observations, **(b)** Model standard *dust* simulations and **(d)** Model *dust_ft* simulations including a forced emission trend. Only statistically significant trends (p value < 0.05) are represented (cf. Sect. 2). All modeling results represent a 3 member's ensemble mean.

ACPD
15, 4879–4907, 2015

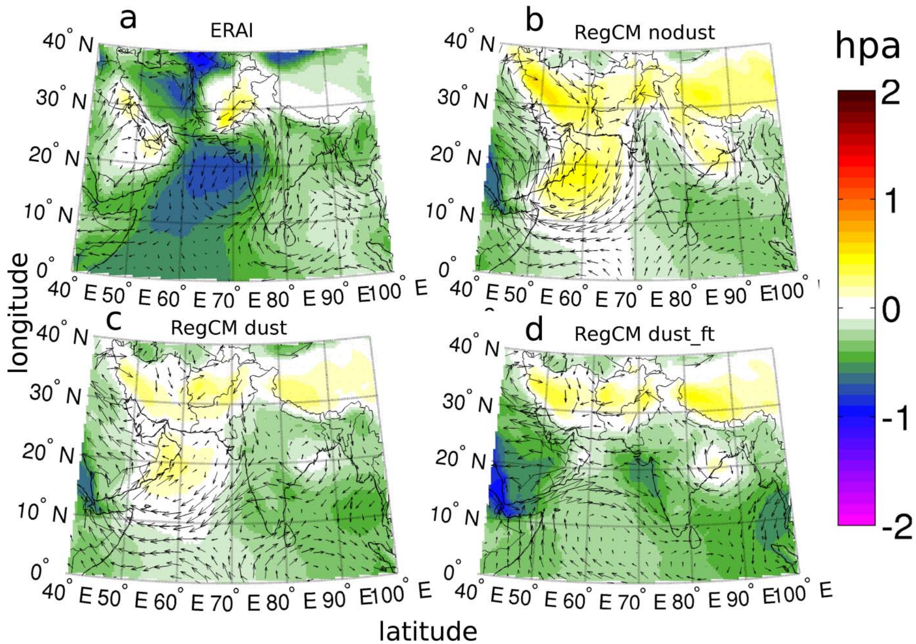

Figure 8. Difference of mean JJAS 850 hPa circulation and surface pressure between "dusty" (2005–2009) and "less dusty" (2000–2004) pentads as defined in the text and calculated from: **(a)** ERAI reanalysis, **(b)** "*nodust*" simulations, **(c)** "*dust*" standard simulations, **(d)** "*dust_ft*" simulations with forced emission trend. As a complement to ERAI, an equivalent graph has been produced from NCEP reanalyzes and displayed in Fig. S7. All simulated results represent a 3 members ensemble mean.

ACPD
15, 4879–4907, 2015

Increasing Arabian dust activity and the Indian Summer Monsoon

F. Solmon et al.